Title:

Structural and magnetic investigation of $In_2Fe_{2-x}Ga_xCuO_7$

Author Affiliations:

Rosa Grajczyk[†], Adam Chan[‡], A. P. Ramirez[‡], and M. A. Subramanian[†]*
[†]Department of Chemistry, Oregon State University, Corvallis, OR 97331
[‡]Department of Physics, University of California Santa Cruz, Santa Cruz, CA 95064

*Corresponding author: mas.subramanian@oregonstate.edu

Full Email Addresses:

Rosa Grajczyk	rabinovr@onid.orst.edu
Adam Chan	admchan@ucsc.edu
Arthur P. Ramirez	apr@soe.ucsc.edu
M. A. Subramanian	mas.subramanian@oregonstate.edu

Corresponding Author:

Mas Subramanian
mas.subramanian@oregonstate.edu
153 Gilbert Hall
Department of Chemistry, Oregon State University
Corvallis, OR 97330 U.S.A

Tel: 1-541-737-8235

Abstract:

The solid solution of $In_2Fe_{2-x}Ga_xCuO_7$ (space group $P6_3/mmc$) was synthesized and investigated through X-ray diffraction and magnetic susceptibility studies. Limited changes to the lattice parameters were observed as a result of the similar ionic radii for Fe^{3+} and Ga^{3+} in the trigonal bipyramidal (TBP) crystallographic site. An increase in the Weiss temperature, along with spin glass behavior are observed from $x = 0 – 2$, but irregularities in the trend are apparent for $x = 0.75$ and 1. With the highest concentration in magnetic ions, $In_2Fe_2CuO_7$ appears to have competing nearest neighbor interactions that produce a suppression of the Curie tail and the experimental magnetic moment. In comparison to $InFe_{1-x}Ga_xCuO_4$, both solid solutions show an invariable progression of the lattice parameters, but the magnetic properties are greatly affected by the distinct TBP layering schemes.

Keywords: Layered compounds, transition metal oxides, trigonal bipyramidal coordination, X – ray diffraction, magnetic properties

1. Introduction

The crystal structure of $LnFe_2O_4$ (space group, $R\bar{3}m$) consists of alternating layers of LnO_6 octahedra and a double layer of FeO_5 trigonal bipyramids (TBP), with an average charge of $Fe^{2.5+}$ (Figure 1) [1–4]. It is well known that deviations in stoichiometry, most specifically from oxygen deficiencies that control the ratio of Fe^{3+} and Fe^{2+}, control the charge ordering and other important properties such as multiferroelectricity in these materials [5–7]. In an effort to understand the electronic interactions that occur through the TBP layers, a large number of alternative tri- and divalent cations have been substituted into the TBP site for Fe [4,5,8–14]. Additional layering schemes were also studies for a deeper understanding of the TBP coordination, leading to compositions such as $Yb_2Fe_3O_7$, $Yb_3Fe_4O_{10}$, and $InFeO_3(ZnO)_m$ (m = 1 – 9) [2,4,11–20].

Similar to the structure of $LnFe_2O_4$, the $Yb_2Fe_3O_7$ structure can be described as a layering of YbO_6 octahedra and FeO_5 trigonal bipyramids, with the presence of two different iron environments, shown in Figure 1 [21,22]. This compound was discovered by Kimizuka *et al.* in 1974, but because of the complex interactions of the iron in two types of TBP layers, the true structure of the material was not determined until the independent work of Kato *et al.* and Malaman *et al.* [21–23]. Kato *et al.* most clearly described $Yb_2Fe_3O_7$ (space group, $P6_3/mmc$) as alternating layers of $YbO_{3/2}$, $FeO_{3/2}$ and $Fe_2O_{5/2}$, where a single TBP layer containing Fe^{3+} was present in addition to the double TBP layer of $Fe^{3+/2+}$ [21]. The charge ordering of this material and that of analogous compositions has led to multiple reports of competing magnetic interactions through two types of ordering, one that occurs within the TBP layer and one that occurs along the *c* axis, [6,24–26]. As with $LnFe_2O_4$, alternative tri- and divalent cations have been substituted in the $Yb_2Fe_3O_7$ structure with the goal of rationally designing enhanced

materials [4,11,12,14,25,27]. Unfortunately, only the structural relationships of the parent compounds with respect to Vegard's Law have been addressed for most of the compositions [4,11,12,14,27]. Qin *et al.* compared the effects of Mg^{2+} on both the structural and physical properties of $LuFe_2O_4$ and $Lu_2Fe_3O_7$, and determined that, while the addition of Mg^{2+} suppressed charge and spin ordering in both systems, the effect in $LuFe_2O_4$ was greater [25].

An extensive discussion of the compounds in the $R_2O_3 – M_2O_3 – M'O$ system (R = In, Sc, Y, *Ln*; M = Fe, Ga, Al; M' = divalent cation) was provided by Kimizuka *et al.*, where the vast number of compositions is compared on the basis of cation substitutions and crystal structure [4]. Although a large number of compositions have been synthesized, a limited amount of information has been reported concerning the structure/property relationships of compounds where In^{3+} is in the *Ln* site, with the exception of possible transparent conducting oxides [28–30]. The initial structural discussion of these compositions was completed by Kimizuka *et al.*, [11,12,14] but only recently have the structure/property relationships of these materials been investigated [28,30–35]. To the best of our knowledge, the first and only structural discussion of the $In_2Fe_2CuO_7$ and $In_2FeGaCuO_7$ compositions was provided by Kimizuka *et al.*, but the physical properties were not reported [11]. In this work $(InFeO_3)_nCuO$ (n = 1 – 3) was determined to be isostructural to $(YbFeO_3)_nCuO$ (n = 1 – 3), and the similarity of radius and bonding between Fe^{3+} (0.55 Å) and Ga^{3+} (0.58 Å) in the TBP site allowed for the additional compositions of $In_2FeGaCuO_7$ and $In_2Ga_2CuO_7$ to be discovered [11,36]. Each of these compositions possess layers of the InO_6 octahedra layer alternating with a double layer of $(Fe^{3+}/Ga^{3+}/Cu^{2+})O_5$ TBP and a single layer of $(Fe^{3+}/Ga^{3+})O_5$ TBP [4,11,12].

A comparison of the structural and transport properties of $InGaCuO_4$ and $In_2Ga_2CuO_7$ was performed by Cann *et al.*, where the transport data showed these materials to be

semiconductors with a band gap determined by an activation energy of 0.50 eV, but the issue of a magnetic ground state was not addressed [32]. We address this question in the present study, building on our recent work showing that a complete solid solution, $InFe_{1-x}Ga_xCuO_4$, can be produced [35]. Although the structural parameters across the solid solution are weakly varying, the interpretation of the magnetic ground state was found to be simplified through the dilution of the magnetic Fe^{3+} [35].

In order to understand the relationship between the structure and magnetic interactions, we have measured the magnetic susceptibility of the substitutional series of $In_2Fe_2CuO_7$ with non-magnetic Ga^{3+} replacing Fe^{3+}. We also compare the behavior of $In_2Fe_{2-x}Ga_xCuO_7$ to that of the related system $InFe_{1-x}Ga_xCuO_4$.

2. Experimental

Polycrystalline samples of $In_2Fe_{2-x}Ga_xCuO_7$ ($x = 0 – 2$) were prepared using standard solid state reactions with In_2O_3 (99.99%), Ga_2O_3 (99.999%), Fe_2O_3 (99.99%) and CuO (99.99%). To synthesize the compositions of $In_2Fe_{2-x}Ga_xCuO_7$ ($x = 0 – 1$), stoichiometric amounts of each oxide were intimately mixed under ethanol, pelletized, and then heated at 1050 °C for 48 h with intermediate grindings. The compositions of $In_2Fe_{2-x}Ga_xCuO_7$ ($x = 1.25 – 2$) were synthesized using equivalent procedures, but a reaction temperature of 1200 °C were required for phase purity.

Powder X-ray diffraction (XRD) data were obtained on all samples with a RIGAKU MINIFLEX II diffractometer over 5 – 80° 2θ using Cu K_α radiation and a graphite monochromator on the diffracted beam. Polycrystalline silicon (99.999%), $a_0 = 5.4301$ Å, was used as an internal standard for precise lattice determination. Lattice parameters were refined

through the Le Bail method using the GSAS software and EXPGUI user interface [37,38]. Zero field cooled (ZFC) DC magnetization data were collected on all samples with a Quantum Design Physical Properties Measurement System (PPMS) using the ACMS mode with a magnetic field of 0.5 Tesla from 5 to 300 K. Additional measurements of the ZFC and field-cooled (FC) magnetization were performed with a Quantum Design Superconducting Quantum Interference Device (SQUID) magnetometer, in order to characterize the hysteresis associated with spin glass behavior.

3. Results and Discussion

3.1 X-ray diffraction of $In_2Fe_{2-x}Ga_xCuO_7$

The XRD patterns for $In_2Fe_{2-x}Ga_xCuO_7$ are provided in Figure 2 and the results of the Le Bail refinement for each composition are provided in Table 1 and Figure 3. For all compositions, the diffraction peaks for the entire pattern can be refined using the space group $P6_3/mmc$ with no apparent impurity phases, indicating that a complete solid solution has been synthesized. Given the similar ionic radii of Fe^{3+} (0.58 Å) and Ga^{3+} (0.55 Å), there is only a slight decrease in the *a* and *c* lattice parameters from $x = 0 – 2$ [36]. The literature values reported by Kimizuka *et al.* are also provided in Table 1, and there is good agreement between the studies for $In_2Fe_2CuO_7$, $In_2FeGaCuO_7$ and $In_2Ga_2CuO_7$. A comparison of the *c/a* ratios, provided in the inset of Figure 3, shows a linear trend representative of a complete solid solution, and a positive relationship as Ga^{3+} is substituted for Fe^{3+}. This positive relationship indicates that the *c* lattice parameter is more greatly affected by the addition of Ga^{3+}, and although minor, this outcome could be the result of changes in the axial bond lengths while the equatorial bond lengths are fairly constant.

3.2 Magnetic investigation of $In_2Fe_{2-x}Ga_xCuO_7$

Zero-field cooled DC-susceptibility (χ) was measured for all samples from 5 – 300 K, and χ(T) and $1/\chi$(T) are provided in Figures 4 and 5. From the high temperature region of the $1/\chi$(T) data (200 – 300 K), the Weiss constant (θ_w) and effective magnetic moment ($\mu_{eff.}$) of each composition was determined and is provided in Table 2. For compositions of $x = 0 – 1$, χ(T) shows an onset of a moment with the increase in Ga^{3+} concentration, but there is a decrease in the moment for compositions of Ga^{3+} greater than $x = 1$. In Figure 6, zero-field-cooled (ZFC) and field-cooled (FC) magnetization data are shown for the samples $x = 0.0$ to $x = 1.5$. We associate the hysteresis between ZFC and FC data in $\chi(T)$ with spin glass (SG) freezing. The fraction of spins involved in SG freezing, represented by the ratio of the ZFC-FC difference to the total moment at the lowest temperature is on the order of 1%, and thus is not representative of the collective behavior of the majority of spins. The freezing temperature, T_f, indicated by the arrows in the figure, tracks the Fe-concentration, suggesting that the frozen moment derives mainly from the Fe spins. The effective ($\mu_{eff.}$) and theoretical ($\mu_{th.}$) magnetic moments of each composition are provided in Table 2 and Figure 7, where $\mu_{th.}$ were calculated per formula unit using the spin values for 5-fold coordinated high-spin Fe^{3+} (d^5, S = 5/2) and Cu^{2+} (d^9, S = 1/2). The dilution of magnetic Fe^{3+} with the addition of Ga^{3+} is observed through a decrease in $\mu_{eff.}$, but compositions with high Fe^{3+} content show a deviation from the theoretical magnetic moment as a result of competing nearest neighbor interactions. We note that our calculation of $\mu_{eff.}$ assumes the same θ_w for the Fe- and Cu-derived spins, which is not required in the case of arbitrary coupling between the two sublattices. In the present case, however, the reasonably good agreement between $\mu_{eff.}$ and $\mu_{th.}$ suggests the validity of this approximation and in particular

a strong coupling between the Fe and Cu sublattices in the strongly paramagnetic temperature region.

It is apparent that θ_w increases with Ga^{3+} concentration, shown in Figure 8, from θ_w = -891 K for x = 0 to θ_w = -3 K at x = 2. This trend can be understood qualitatively by the dilution of magnetic ions in the TBP site, where ferromagnetic interactions between the single and double TBP layers would reduce the antiferromagnetic mean field within the double layer. Irregularities in this trend are observed for x = 0.75 and 1, where the ferromagnetic interaction seems to dominate. We note however, that for these compositions, the $1/\chi$ data deviate from the fit at a higher temperature, suggesting the onset of short-range correlations at a higher temperature. The observed lack of a long range order feature in χ(T), in addition to the systematic progression of θ_w suggest that the Fe-Fe interactions are mainly responsible for the mean field and that these interactions are frustrated in producing long range magnetic order, which is not surprising given the triangular symmetry of the lattice.

3.3 Comparison of $In_2Fe_{2-x}Ga_xCuO_7$ and $InFe_{1-x}Ga_xCuO_4$ Solid Solutions

As shown in Figure 1, the crystal structures of $InFe_{1-x}Ga_xCuO_4$ and $In_2Fe_{2-x}Ga_xCuO_7$ can be described as variations of $(InMO_3)_n(M'O)_m$, where M = Fe^{3+}/Ga^{3+} and M' = Cu^{2+}. When (n + m) equals an even value, such as with $InFeCuO_4$, the compound crystallizes into the non-centro-symmetric space group $R\bar{3}m$ and contains a double layer of the $(M/M')O_5$ TBP [4]. Conversely, when (n+m) equals an odd value, such as with $In_2Fe_2CuO_7$, and additional single TBP layer is introduced into the structure and the centro-symmetric $P6_3/mmc$ space group is obtained [4]. In agreement with this study, the solid solution of $InFe_{1-x}Ga_xCuO_4$ was shown to have limited structural alterations as Ga^{3+} is substituted for Fe^{3+}, regardless of the layering schemes that result

in different space groups [35]. The parallel substitution of Ga^{3+} for Fe^{3+} in both crystal structures confirms that the structural relationships of the TBP crystallographic site in these materials are independent of the layering scheme.

The variations in symmetry produced from the alternative layering schemes is not only observed in the diffraction patterns of these materials, but also through differences in the magnetic interactions of each solid solution. Difficulties in determining the magnetic ground state of $InFeCuO_4$ have previously been discussed, where thermal remnant magnetization pointed towards ferrimagnetism, but a shift in the AC susceptibility indicated spin glass behavior [35,33]. Spin glass behavior was also discussed for $InFe_{1-x}Ga_xCuO_4$ [35]. In the present study, SG-like freezing of spins is seen, without evidence of long range antiferromagnetic ordering.

For both solid solutions, there is an increase in θ_w as Ga^{3+} is substituted for Fe^{3+} in addition to an anomaly of that trend at $In_2FeGaCuO_7$ and $InFe_{0.6}Ga_{0.4}CuO_4$. As shown in Figure 9, the gradual increase in ferromagnetic interactions is observed for both $InFe_{1-x}Ga_xCuO_4$ and $In_2Fe_{2-x}Ga_xCuO_7$, but the irregularity near 50% Fe^{3+} is less extreme for $InFe_{1-x}Ga_xCuO_4$. The large positive θ_w for $In_2FeGaCuO_7$ demonstrates a dominant ferromagnetic interaction between the single and double TBP layers. The absence of the single layer in $InFe_{1-x}Ga_xCuO_4$ results in fewer ferromagnetic bonds, producing a more linear relationship of θ_w with x. The interactions between the TBP layers also influence the $\mu_{eff.}$ in these materials, shown in Figure 10. As described, the deviations observed for $In_2Fe_{2-x}Ga_xCuO_7$ could be credited to nearest neighbor interactions. For $InFe_{1-x}Ga_xCuO_4$, much less deviation from $\mu_{th.}$ is observed, attesting to the increased magnetic frustration produced by the additional single TBP layer in $In_2Fe_{2-x}Ga_xCuO_7$.

4. Conclusions

The $In_2Fe_{2-x}Ga_xCuO_7$ solid solution (space group $P6_3/mmc$) has been successfully produced and investigated through X-ray diffraction and magnetic susceptibility studies. As a result of the similar ionic radii for Fe^{3+} and Ga^{3+} in the TBP site, there was little variation in the *a* and *c* lattice parameters observed across the compositional range. The magnetic susceptibility indicates that this frustrated system has a small concentration of frozen spins (approximately 1%) leading to freezing temperatures that track the concentration of Fe^{3+}. The increasing θ_w across the solid solution agrees with the dilution of the magnetic Fe^{3+}, but the irregularities in this trend at $x = 0.75$ and 1 should be studied further. A comparison of the $InFe_{1-x}Ga_xCuO_4$ and $In_2Fe_{2-x}Ga_xCuO_7$ solid solutions indicate that the additional single TBP layer significantly changes the magnetic properties of this material, but it does not affect the progression of the structural parameters.

Acknowledgements:

The authors would like to thank Dr. A. W. Sleight and Dr. Romain Berthelot for fruitful discussions concerning this work. This work was supported by NSF Grant DMR 0804167.

References

[1] N. Kimizuka, A. Takenaka, Y. Sasada, T. Katsura, Solid State Comm. 15 (1974) 1321–1323.
[2] N. Kimizuka, T. Katsura, J. Solid State Chem. 15 (1975) 151–157.
[3] N. Kimizuka, T. Katsura, J. Solid State Chem. 13 (1975) 176–181.
[4] N. Kimizuka, E. Takayama-Muromachi, in:, Handbook on the Physics and Chemistry of Rare Earths, Elsevier Science Publishers, 1990, pp. 283–384.
[5] N. Kimizuka, E. Takayama, J. Solid State Chem. 40 (1981) 109–116.
[6] M. Tanaka, Nuclear Instruments and Methods in Physics Research B76 (1993) 149–155.
[7] M.A. Subramanian, T. He, J. Chen, N.S. Rogado, T.G. Calvarese, A.W. Sleight, Adv. Mat. 18 (2006) 1737–1739.
[8] V. Kutoglu, A. Roesler, D. Reinen, Z. Anorg. Allg. Chem. 456 (1979) 130–146.
[9] A. Roesler, D. Reinen, Z. Anorg. Allg. Chem. 479 (1981) 119–124.
[10] N. Kimizuka, E. Takayama, J. Solid State Chem. 41 (1982) 166–173.
[11] N. Kimizuka, E. Takayama, J. Solid State Chem. 53 (1984) 217–226.
[12] N. Kimizuka, T. Mohri, J. Solid State Chem. 60 (1985) 382–384.
[13] N. Kimizuka, T. Mohri, Y. Matsui, K. Siratori, J. Solid State Chem. 74 (1988) 98–109.
[14] N. Kimizuka, T. Mohri, J. Solid State Chem. 78 (1989) 98–107.
[15] N. Kimizuka, K. Kato, I. Shindo, I. Kawada, T. Katsura, Acta Cryst. B32 (1976) 1620.
[16] Y. Matsui, K. Kato, N. Kimizuka, S. Horiuchi, Acta Cryst. B35 (1979) 561–564.
[17] Y. Matsui, J Appl Crystallogr 13 (1980) 395–397.
[18] N. Kimizuka, A. Yamamoto, H. Ohashi, T. Sugihara, T. Sekine, J. Solid State Chem. 49 (1983) 65–76.
[19] N. Kimizuka, T. Mohri, M. Nakamura, J. Solid State Chem. 81 (1989) 70–77.
[20] N. Kimizuka, T. Mohri, M. Nakamura, J. Solid State Chem. 87 (1990) 449–455.
[21] K. Kato, I. Kawada, N. Kimizuka, I. Shindo, T. Katsura, Z. Kristallogr. 143 (1976) 279–284.
[22] B. Malaman, O. Evrard, N. Tannières, A. Courtois, J. Protas, Acta Cryst. 32 (1976) 749–752.
[23] N. Kimizuka, A. Takenaka, Y. Sasada, T. Katsura, Solid State Comm. 15 (1974) 1199–1201.
[24] J. Iida, M. Tanaka, S. Funahashi, J. Mag. Mag. Mat. 104-107 (1992) 827–828.
[25] Y.B. Qin, H.X. Yang, Y. Zhang, H.F. Tian, C. Ma, Y.G. Zhao, R.I. Walton, J.Q. Li, J. Phys.: Condens. Matter 21 (2009) 015401.
[26] Y.B. Qin, H.X. Yang, L. Wang, H.F. Tian, C. Ma, Y. Li, H.L. Shi, J.Q. Li, Eur. Phys. J. B 75 (2010) 231–236.
[27] K. Siratori, N. Kimizuka, J. Solid State Chem. 99 (1992) 243–257.
[28] M. Orita, H. Tanji, M. Mizuno, H. Adachi, I. Tanaka, Phys. Rev. B 61 (2000) 1811–1816.
[29] I. Kang, C. Park, J. of Korean Phys. Soc. 56 (2010) 476–479.
[30] A. Murat, J. Medvedeva, Phys. Rev. B 85 (2012) 155101.
[31] R.J. Cava, A.P. Ramirez, Q. Huang, J.J. Krajewski, J. Solid State Chem. 140 (1998) 337–344.
[32] D.P. Cann, R. Martin, C. Taylor, N. Vittayakorn, Mat. Lett. 58 (2004) 2147–2151.

[33] K. Yoshii, N. Ikeda, Y. Okajima, Y. Yoneda, Y. Matsuo, Y. Horibe, S. Mori, Inorg. Chem. 47 (2008) 6493–6501.
[34] R. Grajczyk, K. Biswas, R. Berthelot, J. Li, A.W. Sleight, M.A. Subramanian, J. Solid State Chem. 187 (2012) 258–263.
[35] R. Grajczyk, R. Berthelot, S. Muir, A.W. Sleight, M.A. Subramanian, J. Solid State Chem. 199 (2013) 102–108.
[36] R.D. Shannon, Acta Cryst A 32 (1976) 751–767.
[37] A.C. Larson, R.B. Von Dreele, Los Alamos National Laboratory Report LAUR 86-748 (1994).
[38] B.H. Toby, J. Appl. Cryst. 34 (2001) 210–213.

Tables.

Table 1.
Lattice Parameters of $In_2Fe_{2-x}Ga_xCuO_7$ ($x = 0 – 2$) determined through Le Bail refinements of PXRD. Literature values for $x = 0$, 1, and 2 are provided from Kimizuka *et al.* [11].

[x]	a (Å)	c (Å)
0	3.3535(1)	28.842(2)
0 [11]	3.3515(2)	28.871(3)
0.25	3.3511(1)	28.835(2)
0.50	3.3513(1)	28.820(2)
0.75	3.3463(1)	28.796(2)
1	3.3461(1)	28.794(3)
1 [11]	3.3421(2)	28.817(3)
1.25	3.3454(2)	28.792(3)
1.50	3.3421(1)	28.794(2)
1.75	3.3396(1)	28.758(2)
2	3.3332(1)	28.741(2)
2 [11]	3.3319(1)	28.697(2)

Table 2.
Curie-Weiss parameters of $In_2Fe_{2-x}Ga_xCuO_7$ from ZFC DC-susceptibility measurements.

[x]	θ_w (K)	$\mu_{eff.}$ (μ_B)	$\mu_{th.}$ (μ_B)
0.00	-892	9.10	11.97
0.25	-523	9.28	10.50
0.50	-334	8.79	9.05
0.75	-15	6.05	7.60
1.00	85	4.63	6.17
1.25	-183	4.00	4.77
1.50	-143	4.06	3.43
1.75	-66	3.14	2.28
2.00	-3	1.75	1.73

Figure Captions:

Figure 1.
Crystal structure of (a) $YbFe_2O_4$ and (b) $Yb_2Fe_3O_7$. Both structures are comprised of single YbO_6 octahedra layers (grey) alternating with $(Fe^{3+}/Fe^{2+})O_5$ trigonal bipyramids (red).

Figure 2.
XRD patterns for selected compositions of $In_2Fe_{2-x}Ga_xCuO_7$. The evolution of the diffraction peaks indicates that there is a complete solid solution between the hexagonal $In_2Fe_2CuO_7$ and $In_2Ga_2CuO_7$ phases.

Figure 3.
Le Bail refinements of the hexagonal *a* and *c* lattice parameters for $In_2Fe_{2-x}Ga_xCuO_7$ compared to an internal Si standard. The small negative slope verifies that there is only a slight change in the crystal structure when Ga^{3+} is substituted for Fe^{3+}. Inset: The *c/a* ratio follows an expected linear trend for a solid solution.

Figure 4.
ZFC DC-susceptibility for $In_2Fe_{2-x}Ga_xCuO_7$ ($x = 0 – 1$), measured with an applied magnetic field of 0.5 Tesla (a) χ(T) and (b) $1/\chi$(T).

Figure 5.
ZFC DC-susceptibility for $In_2Fe_{2-x}Ga_xCuO_7$ ($x = 1 – 2$), measured with an applied magnetic field of 0.5 Tesla (a) χ(T) and (b) $1/\chi$(T).

Figure 6.
Temperature dependence of zero-field-cooled (ZFC) and field-cooled (FC) magnetic susceptibility for $In_2Fe_{2-x}Ga_xCuO_7$ ($x = 0 – 2$). For each composition an arrow indicates the freezing temperature (T_f), which is follows the change in Fe^{3+} concentration.

Figure 7.
Magnetic moment dependence for $In_2Fe_{2-x}Ga_xCuO_7$ ($x = 0 – 2$). Nearest neighbor interactions produce deviations in the $\mu_{eff.}$ compared to the $\mu_{th.}$ for compositions with high Fe^{3+} content.

Figure 8.
Weiss temperature dependence for $In_2Fe_{2-x}Ga_xCuO_7$ ($x = 0 – 2$). An increase of the θ_w shows that the dilution of magnetic ions results in possible ferromagnetic interactions between the TBP layers interfering with the antiferromagnetic interactions within the layers.

Figure 9.
Comparison of Weiss temperature dependence for $In_2Fe_{2-x}Ga_xCuO_7$ ($x = 0 – 2$) and $InFe_{1-x}Ga_xCuO_4$ ($x = 0 – 1$) [35]. An irregularity is observed for both solid solutions near 50% Fe^{3+}, but it less apparent for $InFe_{1-x}Ga_xCuO_4$.

Figure 10.

Comparison of magnetic moment dependence for $In_2Fe_{2-x}Ga_xCuO_7$ ($x = 0 – 2$) and $InFe_{1-x}Ga_xCuO_4$ ($x = 0 – 1$) [35]. The difference in Fe^{3+} concentration is observed as a decrease in the moment for $InFe_{1-x}Ga_xCuO_4$, where nearest neighbor interactions do not produce large deviations in the $\mu_{eff.}$ compared to those seen in $In_2Fe_{2-x}Ga_xCuO_7$.

Figure 1.

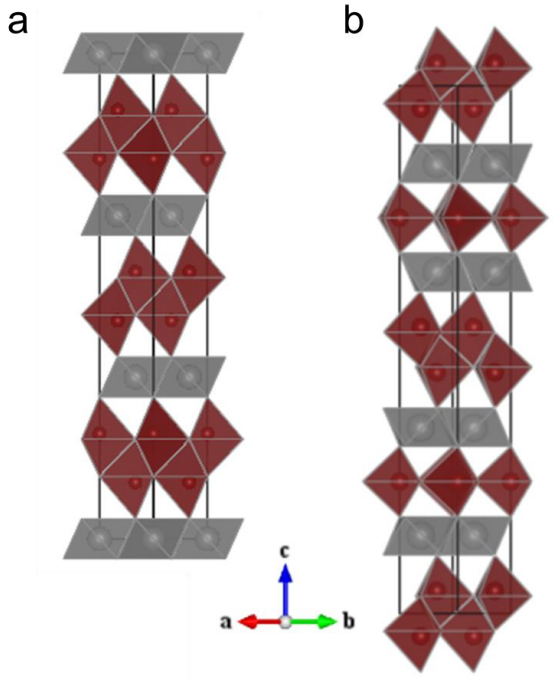

Figure 2.

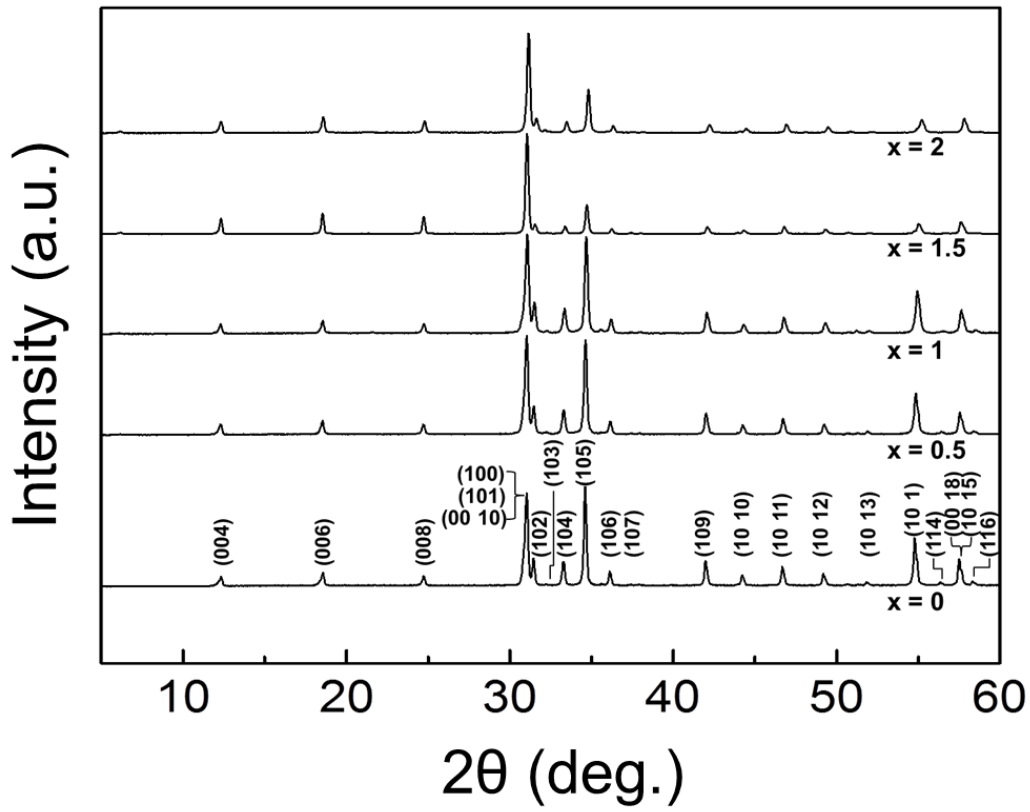

Figure 3.

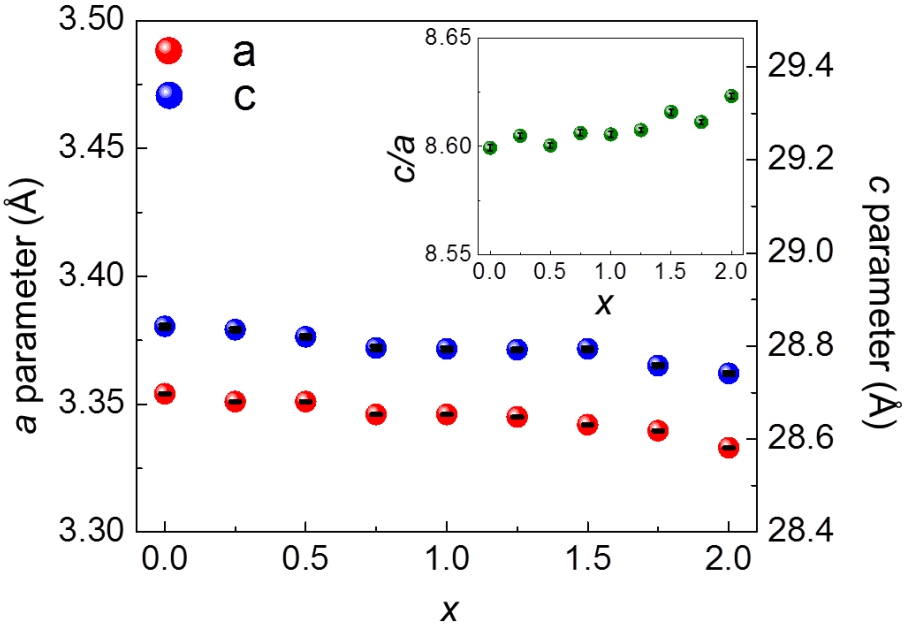

Figure 4.

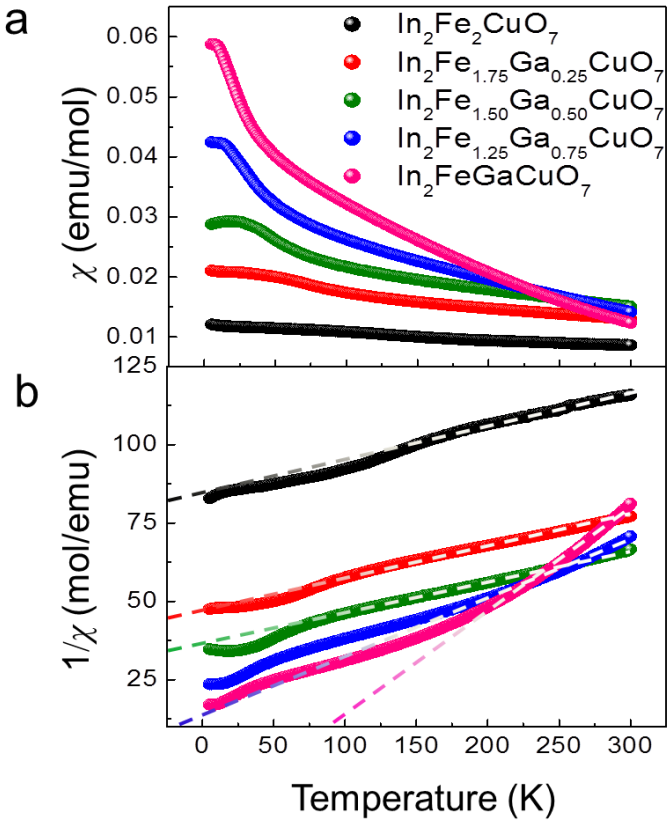

Figure 5.

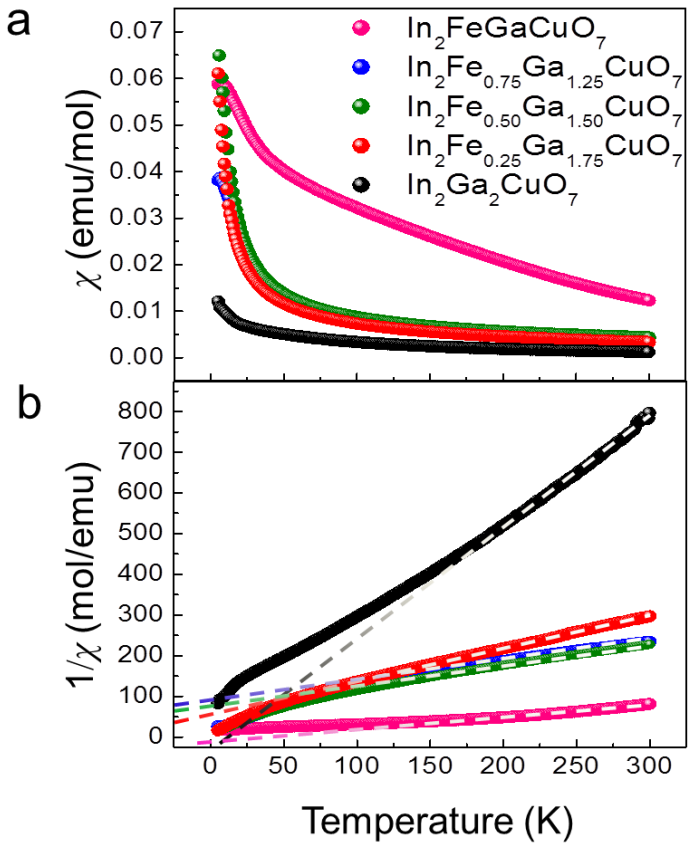

Figure 6.

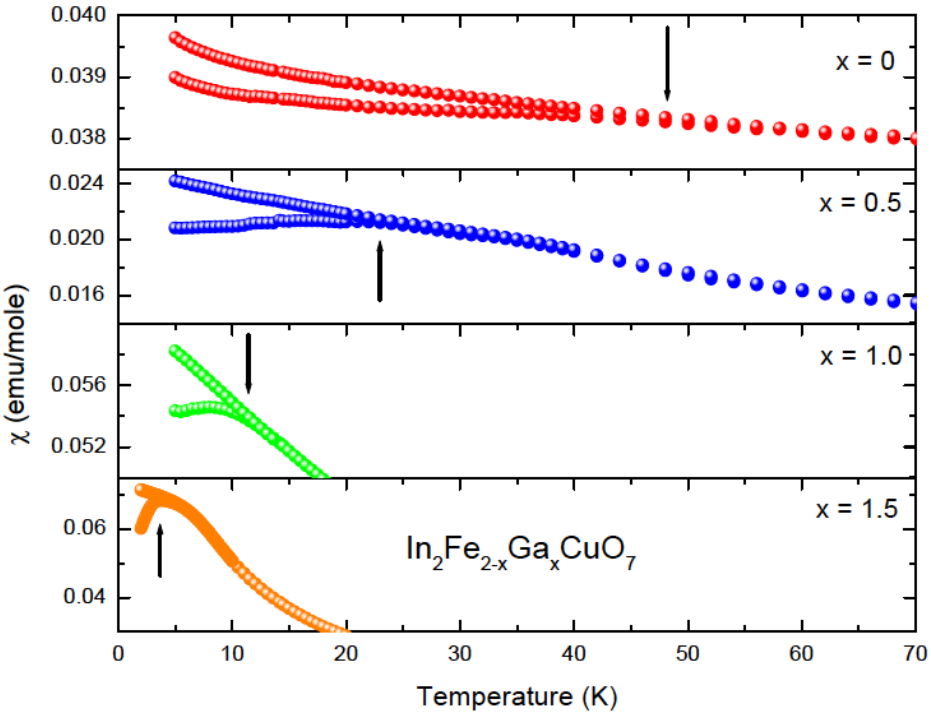

Figure 7.

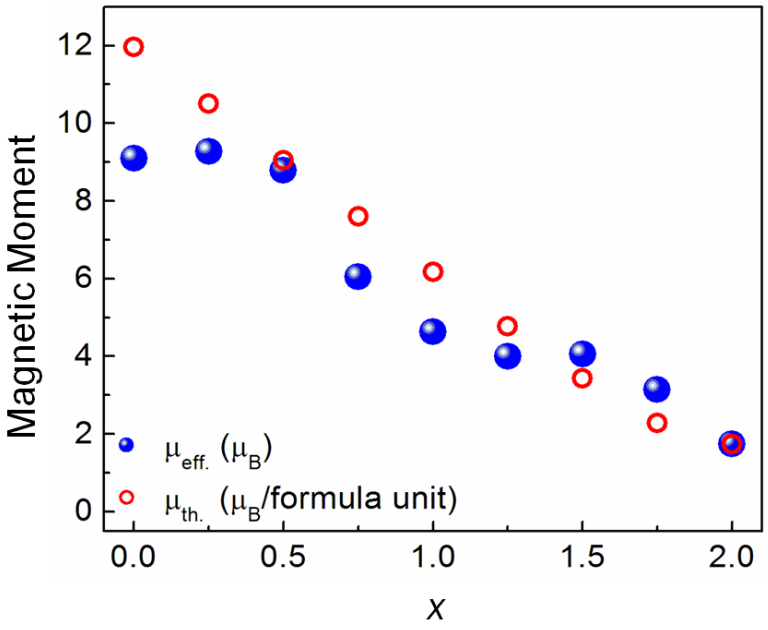

Figure 8.

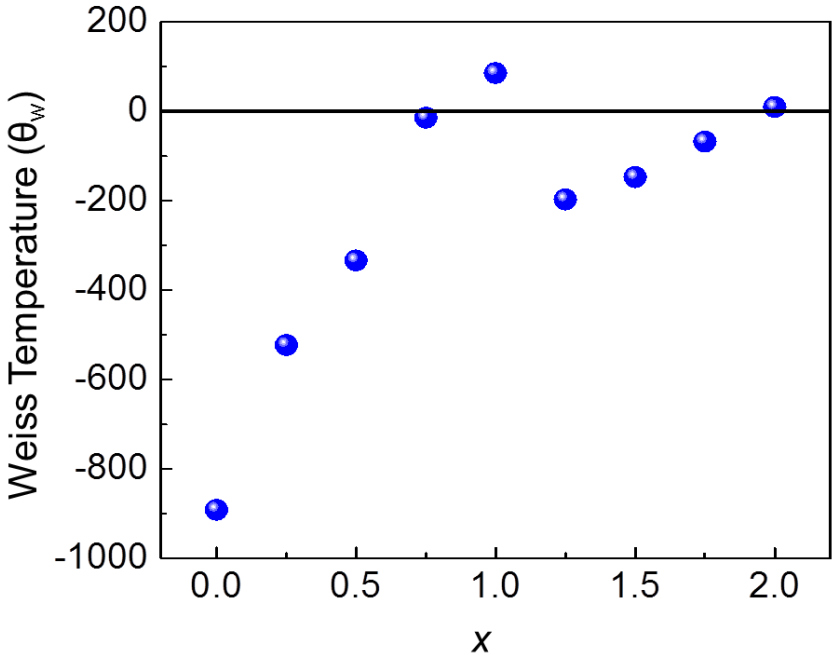

Figure 9.

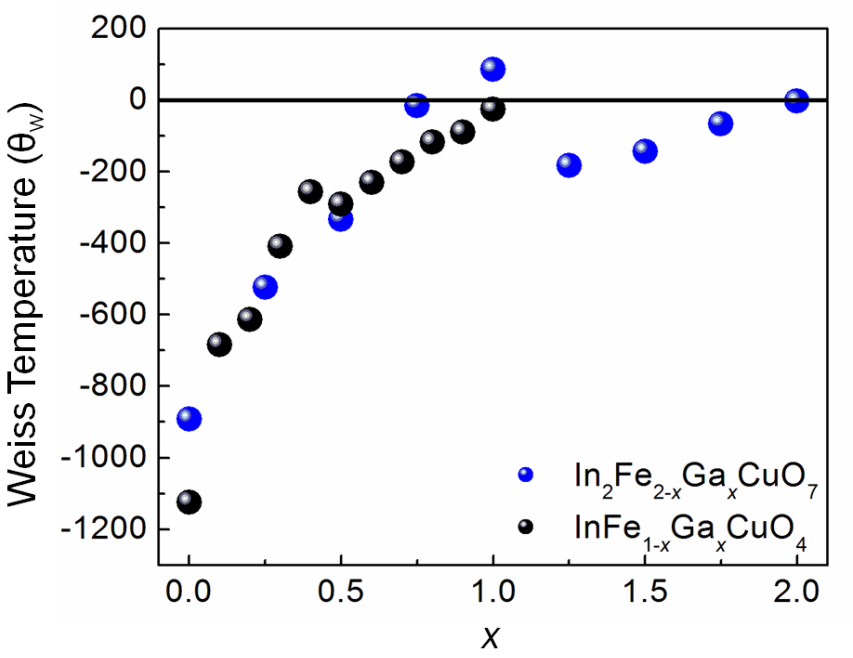

Figure 10.